Journal of Alloys and Compounds 513 (2012) 208–212

Contents lists available at SciVerse ScienceDirect

Journal of Alloys and Compounds

journal homepage: www.elsevier.com/locate/jallcom

The evolution of cold-rolled deformation microstructure of {0 0 1}⟨1 1 0⟩ grains in Ta–7.5 wt%W alloy foils

C. Chen, M.P. Wang*, S. Wang, Y.L. Jia, R.S. Lei, F.Z. Xia, B. Zuo, H.C. Yu

School of Materials Science and Engineering, Central South University, Changsha, 410083, China

ARTICLE INFO

Article history:
Received 26 June 2011
Received in revised form 5 October 2011
Accepted 7 October 2011
Available online 17 October 2011

Keywords:
Cold-rolled
Electron backscattering diffraction
Microbands
Dislocation microstructures

ABSTRACT

The deformation structure of {0 0 1}⟨1 1 0⟩ grains in cold-rolled Ta–7.5 wt%W alloy foils has been investigated by transmission electron microscopy (TEM) and electron backscattering diffraction (EBSD). The results show that there are two kinds of {0 0 1}⟨1 1 0⟩ grains formed during the cold-rolled deformation process. Type A grains are surrounded by α-fiber, while type B grains are surrounded by γ-fiber. Dislocation analysis reveals a continuous evolution of dislocation substructures from dislocation arrays, to high dense dislocation walls, and to microbands in type A grains, while in type B grains from dislocation mesh to dislocation cells as a function of plastic strain. By both the analysis of EBSD and TEM, a new deformation mode in type A grains is developed.

1. Introduction

Ta and Ta–W alloys are used in a number of industrial applications because they provide a good combination of properties, such as high density, excellent formability, high melting point, and a moderately high elastic modulus, etc., which are not found in many other refractory metals [1–11]. Due to these unique features, they have become one of the most promising materials for applications in power, aerospace and nuclear engineering fields [8]. As a result, many available studies were focused on the mechanical behavior of Ta and Ta–W alloys [9,10,11]. However, few researchers have correlated properties with deformation microstructures and crystal orientation in them. Since Ta and Ta–W alloys are bcc materials, the well-developed rolled texture of Ta and Ta–W alloys can be represented as two fibres, α and γ. In α fibre, ⟨1 1 0⟩ parallels the rolling direction and in γ fibre ⟨1 1 1⟩ parallels the rolling plane normal direction [12]. For deformation structure in BCC metals and alloys, there are many articles about steels. For example, many authors have reported that there is a correlation between the deformation microstructure and the crystal orientation in IF steels [13,14,15]. Chen et al. [16] suggested that during cold-rolled deformation, the α fiber grains in IF steels can use as many as seven independent slip systems, which allow homogeneous deformation in them. They also indicated that under such circumstances, dislocation structures in grains belonging to α fiber must constantly evolve during cold deformation, but how they do so remains unclear. It is essential to study microstructure evolution during cold deformation of metals for which is important in its relationship to deformation mechanisms, mechanical properties, and texture formation. Furthermore, the characteristics of deformation microstructures affect the way in which materials behave during recovery and recrystallization. As an important kind of refractory alloy it is important and meaningful to correlate deformation structures with orientation in Ta–W alloys and to study the evolution of the deformed structures during cold rolling process. However, not sufficient attention has been paid on this topic in Ta–W alloys, especially when the strips are very thin. The objective of this article is to investigate how deformation microstructures evolve during cold rolling at medium reduction levels in most common grains of {0 0 1}⟨1 1 0⟩ in Ta–7.5 wt%W alloy foils.

2. Experimental procedure

Ta–7.5 wt%W alloys were prepared by a powder metallurgy method for a fine grain structure in original materials. The sintered plates of 50 μm average grain size were processed by cold rolled to 50% by 10% reduction per pass, and then the plates were annealed at 1473 K for 1 h with a uniformly recovered condition. The annealed plates were cold rolled to 50% again and then annealed at 1473 K for 1 h. By repeating this process, a 150 μm plate was obtained. After annealed at 1473 K for 1 h, the 150 μm plates were cold rolled in the range from 10 to 50% and the deformation microstructure has been analysed by TEM. Since the plates are very thin, TEM observation was conducted on rolling planes with a JEOL 2010 transmission electron microscope. The specimens were twin-jet polished in a mixing solution of HF, H_2SO_4 and CH_3OH with ratio of 1:5:94 at 273 K. EBSD investigations were also done on the rolling planes of the 100 μm foils.

3. Results and discussion

For bcc metals, in the Bunge version of Euler space, the full orientation distribution function needs not be shown because the

* Corresponding author. Tel.: +86 731 8830264; fax: +86 731 8876692.
E-mail address: chench011-33@163.com (M.P. Wang).

0925-8388/$ – see front matter © 2011 Elsevier B.V. All rights reserved.
doi:10.1016/j.jallcom.2011.10.020

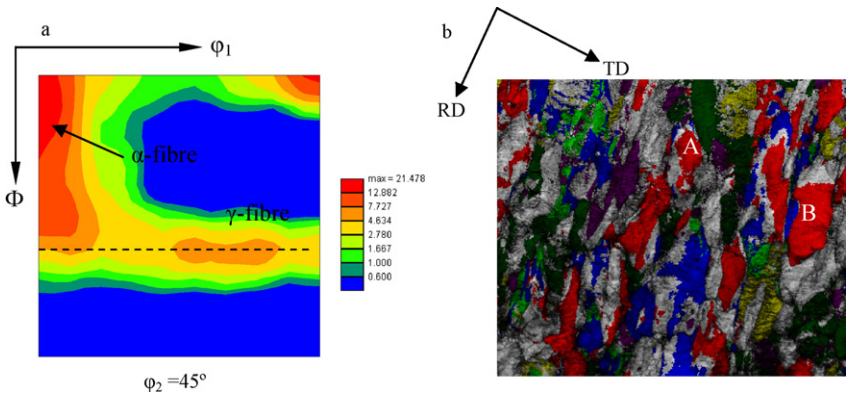

Fig. 1. (a) The φ_2 45° section of ODF maps showing the major components of the α and γ fibers in Ta–7.5 wt%W alloys foils cold-rolled to a reduction of 50%;(b) OIM micrographs showing the major grains distributed in Ta–7.5 wt%W foils, color code in OIM: Red-(0 0 1)[1-1 0], blue-(1 1 2)[1-1 0], green-(1 1 1)[1-1 0], violet-(1 1 1)[1 1-2], deep green-(1 1 1)[0-1 1]. (For interpretation of the references to color in this figure legend, the reader is referred to the web version of the article.)

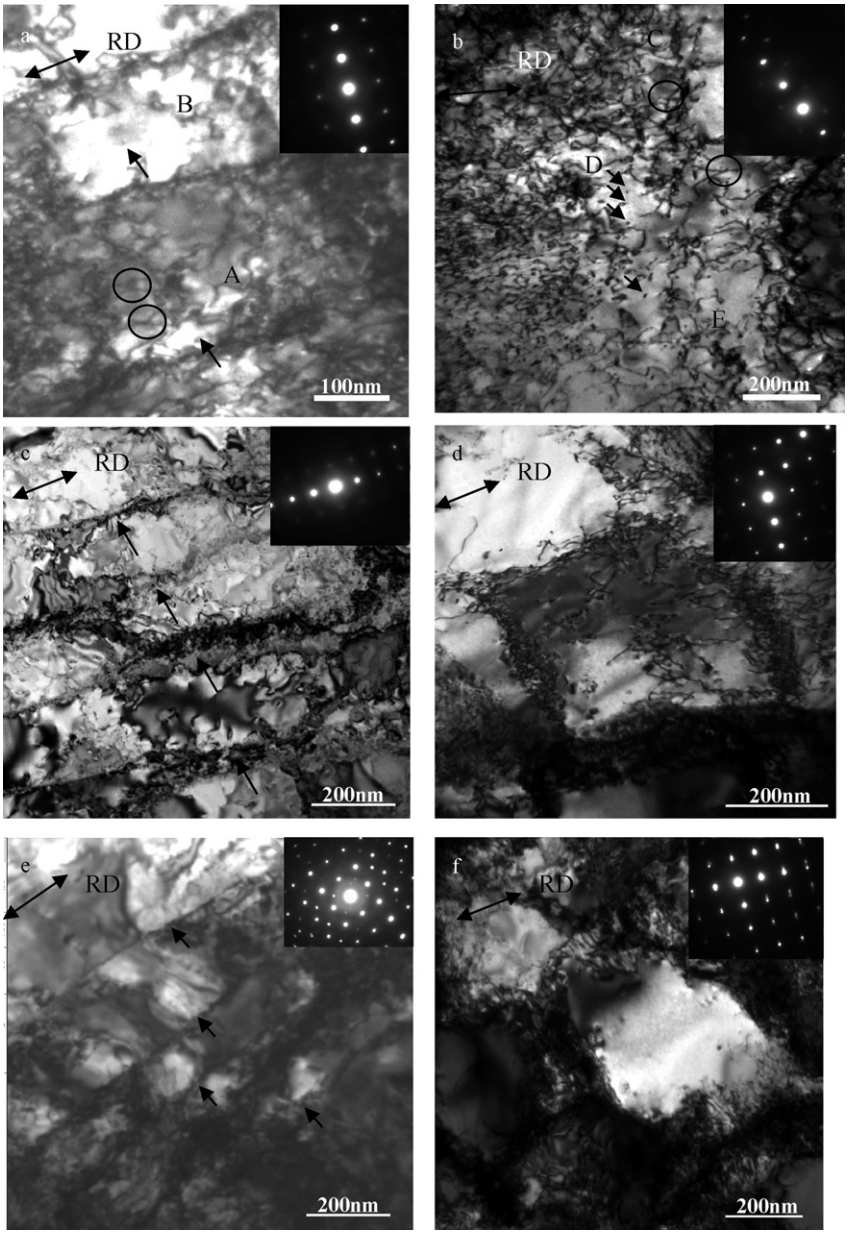

Fig. 2. Typical dislocation structures and the corresponding SADPs of Ta–7.5 wt%W alloy foils. (a), (c) and (e) show the typical deformation structures in type A grains with reductions of 10%, 20% and 50%. (b), (d) and (f) show the typical deformation structures in type B grains with reductions of 10%, 20% and 50%. The rolling direction is marked by RD.

Table 1
Volume fractions of the main texture components in Ta–7.5 wt%W alloy foils.

Color	Orientation	Fraction
Red	(0 0 1) [1-1 0]	0.193
Blue	(1 1 2) [1-1 0]	0.127
Green	(1 1 1) [1-1 0]	0.042
Violet	(1 1 1) [1 1-2]	0.053
Deep-green	(1 1 1) [0-1 1]	0.120

$\varphi_2 = 45^\circ$ section contains sufficient information to allow a proper discussion of the bcc rolling texture, including α and γ fibers [17]. Fig. 1a depicts the deformation textures of Ta–7.5 wt%W alloy cold-rolled to a reduction of 50%. It clearly shows that α and γ fibers are well developed after 50% cold-rolled reduction. The main components in α fiber include {0 0 1}⟨1 1 0⟩, {1 1 2}⟨1 1 0⟩ and {1 1 1}⟨1 1 0⟩, and γ fiber spreads from {1 1 1}⟨1 1 0⟩ to {1 1 1}⟨1 1 2⟩. Fig. 1b shows an EBSD micrograph which shows grains of the major orientation distributed in the foils with different colors. The volume fractions of them are list in Table 1. As shown in Table 1, the fraction of (0 0 1)[1 1 0] reaches 19.3%. There are two types of {0 0 1}<1 1 0> grains marked by A and B in Fig. 1b which are surrounded by γ and α grains, respectively. With the effects of different surroundings, it suggests that these two grains may derive from grains of different orientations and undergo different deformation modes. As a result, the evolution of deformation structure in the type A and B {0 0 1}<1 1 0> grains was carefully investigated herein below.

Fig. 2a and b shows typical dislocation structures of {0 0 1}<1 1 0> grains cold-rolled to a reduction of 10%. Several sets of parallel dislocation arrays can be seen in Fig. 2a, with an average space about 200 nm. However, it is homogeneous deformation structure in type B grains during this period (Fig. 2b). Great deals of tangled dislocations are evenly distributed in the grains and no sign of high dense dislocation walls are appear. Furthermore, there are some typical cold deformation structures of bcc metals in both Fig. 2a and b, such as screw dislocation debris (marked by arrows), dislocation dipoles produced by double cross slips of screw dislocations (marked by capital letters). Besides, a lot of scissors type dislocations are formed by a reaction of two 1/2⟨1 1 1⟩ dislocations (marked by circle). It is reported that both double cross slips and scissors type dislocations are play an important role in the formation of microbands [18].

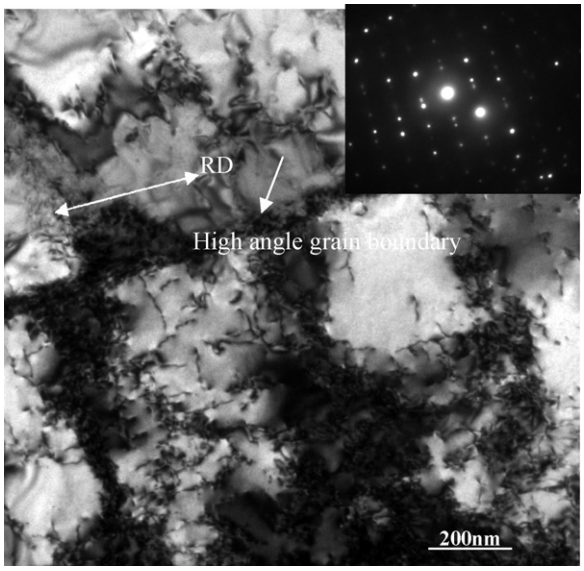

Fig. 3. The cells formed in a type B grain after a reduction of 50% beside the high angle grain boundary. The rolling direction is marked by RD.

Fig. 2c and d shows typical dislocation structures of {0 0 1}⟨1 1 0⟩ grains after a reduction of 20%. Several parallel high dense dislocation walls are formed in type A grains, with an average space of about 200 nm. By trace analysis, it is found that the dislocation walls are parallel to ⟨1 1 0⟩. Therefore, the dislocation walls are formed on {1 1 0} slip planes and the highly activated slip systems are {1 1 0}⟨1 1 0⟩. Fig. 2d shows that the typical dislocation structures formed in type B grains are cells. Dislocations are mainly present in the cell boundaries, while the dislocation density in the cell interiors is very low, where only a few of tangled dislocations can be seen. The diameter d of dislocation cells is on average 500 nm, and the ratio of h/d, where h is the thickness of cell boundaries, is about 0.2. Interestingly, the cell shown in Fig. 2d is nearly a square shape with two sets of walls on different {1 1 0} planes.

Fig. 2e and f shows typical deformed structure in {0 0 1}⟨1 1 0⟩ grains after cold rolled to 50%. As shown in Fig. 2e, a set of microbands is formed in type A grains. Compared with Fig. 2c,

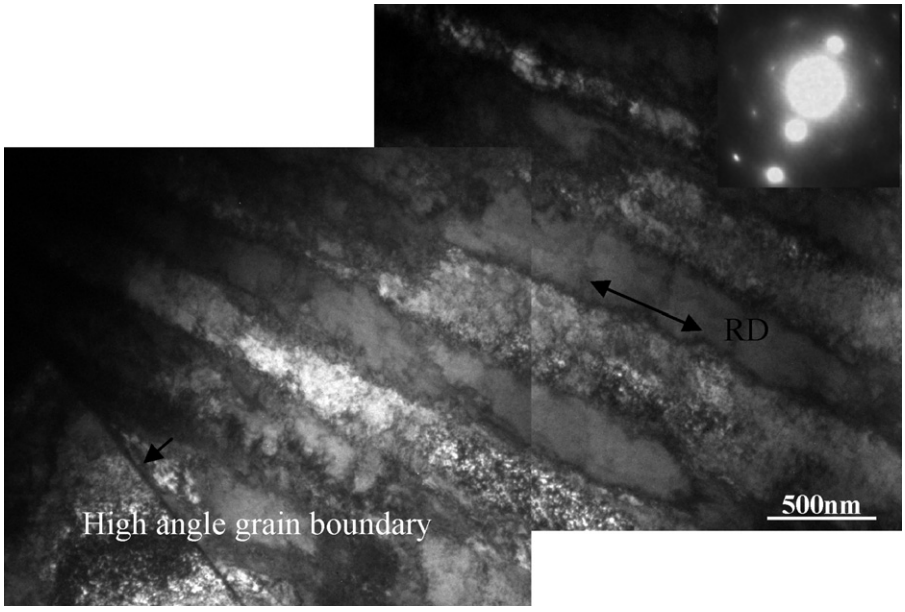

Fig. 4. The microbands formed in a type A grain after a reduction of 50% beside the high angle grain boundary. The rolling direction is marked by RD.

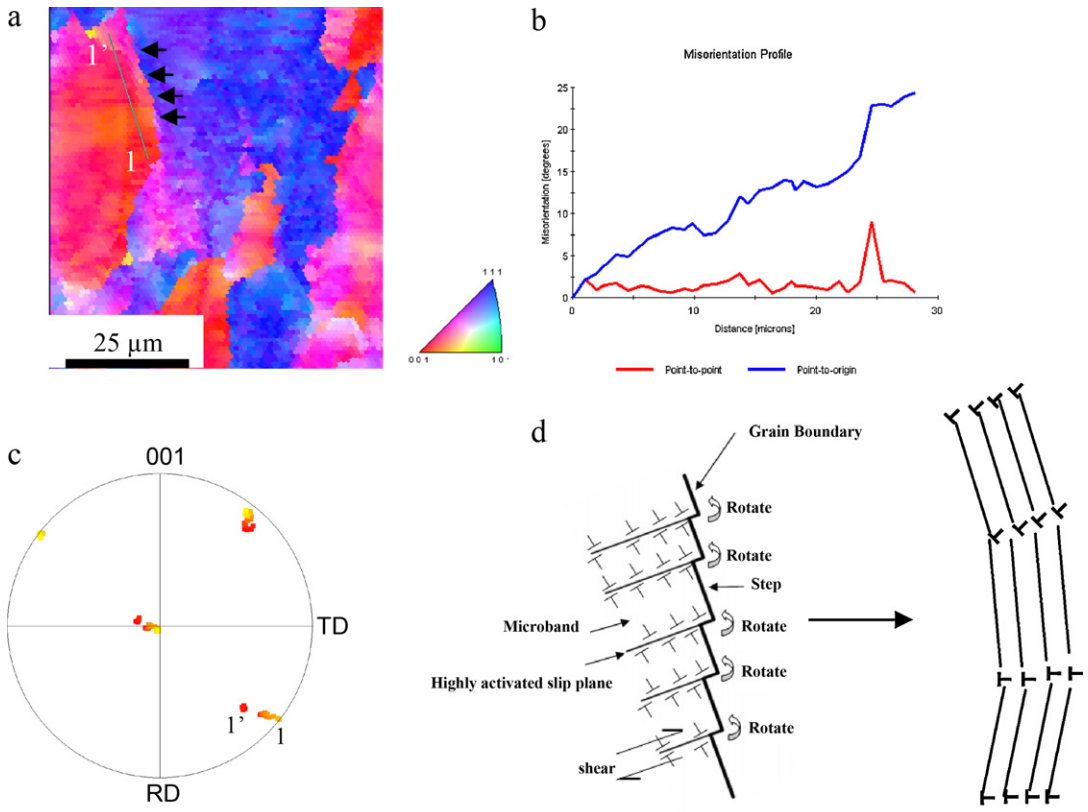

Fig. 5. (a) EBSD generated IPF map of 50% cold-rolled Ta–7.5W foils, (b) The measured misorientations plotted as a function of position along line 11′ in (a), (c). The associated {0 0 1} pole figure. (d) The scheme of formation and rotation of microbands.

the space between these boundaries is 100–200 nm. These boundaries are named as geometrically necessary boundaries (GNBs) after a lot of studies [17,18,19,20]. It is reported that in these high stack fault energy materials, such as Al, Ni, Fe, etc., for a 10–50% rolling reduction, subdivision may occur over several length scales. On a microscopic scale, cell blocks are formed by elongated, planar, approximately parallel GNBs. Within the cell blocks defined by GNBs, individual dislocation cells are delineated by incidental dislocation boundaries (IDBs). Traces of these microbands are located on {1 1 0} planes. The splitting of spots in the corresponding selected area diffraction patterns shows that the angular misorientation across the GNBs is about 2°, which is higher than that in Fig. 2c. The corresponding deformed structures formed in type B grains are shown in Fig. 2f at this deformation condition. Compared with Fig. 2d, it is still a typical cell structure, but with denser dislocations in the wall and less dislocations in the interiors. The cells are about 300 nm in diameter which is smaller than that in Fig. 2d. The misorientation across these boundaries is about 0.5°.

As shown in Fig. 3, there are several cells formed in a type B grain after a reduction of 50% beside the high angle grain boundary. The diameter of dislocation cells is about 300 nm. Meanwhile, Fig. 4 shows the mirobands which are formed beside a high angle boundary in a type A grain. The angle between the high angle boundary and the GNBs is about 25°. The microbands formed in type A grains are also identified by EBSD analysis in Fig. 5. As shown in Fig. 5a, there are several steps formed at the grain boundary (marked by arrows). It is shown in Fig. 5b that total misorientation is accumulated gradually through an additive process. It seems that the misorientation likely results from local differences in stress state within an individual grain. As a result, different parts of the crystal subdivided by GNBs undergo different strains and a continuous rotation of the grain is exhibited. Small variation of misorientations between the neighboring regions across the microbands and it can be confirmed by the {0 0 1} PF showing gentle orientation gradients. The scheme of formation and rotation of microbands is shown in Fig. 5d.

Based on our observation and analysis, we believe that there are mainly two kinds of $\{0\,0\,1\}\langle 1\,1\,0\rangle$ grains which experience different deform modes during the cold-rolled process in Ta–7.5 wt%W alloy foils. It is found that dislocation substructures evolve from dislocation arrays, to high dense dislocation walls and then to microbands in type A grains, while in type B grains, dislocation mesh is formed firstly followed by dislocation cells during the deformation process. It seems that different combinations of the slip systems are activated in the two type grains. It is well known during cold rolling, dislocation glide will force the slip planes to rotate towards the tensile axis due to the constraint of the axis, and the rotation axis is $[h\,k\,l]\times[u\,v\,w]$, where $[h\,k\,l]$ is the normal of the slip plane and $[u\,v\,w]$ is the slip direction. By analysis of traces, the rotation axis is <1 1 2> in this article. Besides, the crystal will rotate about the TD axis geometrically. Then, a rotation about ND and/or RD would occur as a result of the influence of surrounding material [21]. The combination rotation axis is different in grain A and B. It means that the two types of $\{0\,0\,1\}\langle 1\,1\,0\rangle$ grains may derive from different oriented grains and undergo different deformation mode during this process. Therefore, the evolution of deformation structures in type A and B grains is different. There are two famous mechanisms for microbands formation, i.e. Jackson's double cross-slip model [22] and Hansen's dense dislocation walls splitting mechanism [23]. Both two mechanisms show that it is essential to form high dense dislocation walls during the formation of microbands. In our study, the microbands are derived from walls of dislocations formed under a limited condition giving

rise to highly concentrated microplastic deformation in the form of dislocation sheets.

4. Conclusions

In summary, by the analysis of EBSD, there are two types of $\{0\,0\,1\}\langle 1\,1\,0\rangle$ grains formed during cold-rolled deformation with different surroundings. The evolution of deformation structure in type A and B grains is quite different. Dislocation analysis reveals a continuous evolution of the dislocation substructures from dislocation arrays, to high dense dislocation walls, and to microbands in type A grains, while in type B grains from dislocation mesh to dislocation cells. By the analysis of EBSD and TEM, a deformation mode is developed in grain A.

Acknowledgement

This work is supported by the "863" Project (2006AA03Z517) of the Ministry of Science and Technology of the People's Republic of China.

References

[1] S. Nemat-nasser, J.B. Issscs, Acta Mater. 45 (1997) 907.
[2] S.N. Mathaudhu, K.T. Hartwig, Mater. Sci. Eng. A 463 (2007) 94.
[3] F. Cao, E.K. Cerreta, C.P. Trujillo, G.T. Gray III, Acta Mater. 56 (2008) 5804.
[4] W. Kock, P. Paschen, JOM 41 (1989) 33.
[5] G.T. Gray III, N.K. Bourne, J.C.F. Millett, J. Appl. Phys. 94 (2003) 6430.
[6] K. Masuda-Jindo, V.V. Hung, N.T. Hoa, P.E.A. Turchi, J. Alloys Compd. 452 (2008) 127.
[7] M.A. Meyers, F.D.S. Marquis, D.S. Kim, Y.J. Chen, Metall. Trans. A 26 (1995) 2493.
[8] G.T. Gray, K.S. Vecchio, Metall. Mater. Trans. A 26 (1995) 2555.
[9] S. Nemat-nasser, R. Kapoor, Int. J. Plast. 17 (2001) 1351.
[10] Z. Lin, E.J. Lavernia, F.A. Mohamed, Acta Mater. 47 (1999) 1181.
[11] C.L. Briant, D.H. Lassila, Trans. ASME 121 (1999) 172.
[12] Y.B. Park, D.N. Lee, Acta Mater. 46 (1998) 3371.
[13] Z.J. Li, G. Winther, N. Hansen, Acta Mater. 54 (2006) 401.
[14] J.J. Jonas, J. Mater Process. Technol. 117 (2001) 293.
[15] M.Z. Quadir, B.J. Duggan, Acta Mater. 52 (2004) 4011.
[16] Q.Z. Chen, M.Z. Quadira, B.J. Duggana, Philos. Mag. 86 (2006) 3633.
[17] M.Z. Quadir, B.J. Duggan, Acta Mater. 54 (2006) 4337.
[18] Q.Z. Chen, B.J. Duggana, Metall. Trans. A 35 (2004) 3423.
[19] N. Hansen, X. Huang, G. Winther, Mater. Sci. Eng. A 494 (2008) 61.
[20] J.A. Wert, Q. Liu, N. Hansen, Acta Metall. Mater. 43 (1995) 4153.
[21] M.Z Quadir, B.J. Duggan, ISIJ Int. 46 (2006) 1495.
[22] P.A. Jackson, Scr. Metall. 17 (1983) 199.
[23] D.A. Hughes, N. Hansen, Mater. Sci. Technol. 7 (1991) 544.